International Journal of Applied Pharmaceutics

ISSN- 0975-7058 Vol 16, Special Issue 6, 2024

Original Article

ANTICANCER STUDIES OF ZERUMBONE-LOADED CHITOSAN-OLEIC ACID NANOPARTICLES AGAINST T47D BREAST CANCER CELLS

ERINDYAH R. WIKANTYASNING*, ZULFA MAZIDAH, MUHAMMAD DA'I, IKA TD KUSUMAWATI, SUPRAPTO SUPRAPTO

Faculty of Pharmacy, Universitas Muhammadiyah Surakarta, Jl. A. Yani 157 Pabelan, Kartasura, Sukoharjo-57169, Indonesia
***Corresponding author: Erindyah R. Wikantyasning; *Email: erindyah.rw@ums.ac.id**

Received: 26 Mar 2023, Revised and Accepted: 15 Sep 2024

ABSTRACT

Objective: The phytochemical compound zerumbone is derived from the rhizome of *Zingiber zerumbet* (L.) Smith. Nanotechnology-based drug delivery system employing chitosan-oleic acid nanoparticles to transport zerumbone. This study aimed to examine the cytotoxic activity of zerumbone nanoparticles against T47D breast cancer cells.

Methods: Using the ionic gelation method, zerumbone-loaded chitosan-oleic acid nanoparticles were synthesized and characterized for particle size, zeta potential, morphology, and encapsulation efficiency. Utilizing the MTT assay, flow cytometry, and confocal microscopy, the cytotoxic activity of nanoparticles was evaluated.

Results: The characterization of zerumbone nanoparticles resulted in a particle size of 116±12.04 nm, polydispersity index of 0.74±0.07 µm, and zeta potential of (+34.4) mV. HPLC analysis showed an encapsulation efficiency of 92.43±1.73%. The uptake of zerumbone-loaded chitosan-oleic acid nanoparticles into T47D cells induced higher apoptosis than the zerumbone isolate and the control nanoparticles.

Conclusion: Zerumbone-loaded chitosan-oleic acid nanoparticles showed anticancer activity against breast cancer cells T47D. Using nanoparticles as a drug delivery system would improve the clinical efficacy of anticancer treatment, which has significant implications for future cancer treatment strategies.

Keywords: Cytotoxic, Nanoparticles, Zerumbone, Chitosan, T47D cells

DOI: https://dx.doi.org/10.22159/ijap.2024.v16s6.TY2036 Journal homepage: https://innovareacademics.in/journals/index.php/ijap

INTRODUCTION

Cancer is a collection of disorders that induce aberrant cell growth and uncontrolled cell spread in the body. Within five years, the incidence of cancer in the world climbed from 1.4 per 1000 people to 1.8 per 1000 people, with surgery and chemotherapy being the most prevalent treatments. Among the female population, breast cancer remains the leading cause of new cancer diagnoses and cancer-related deaths. In 2020, the incidence and mortality of breast cancer were 47.8 and 13.6 ASR per 100,000, respectively [1]. Surgical procedures and chemotherapy, the most prevalent treatment forms, are still only marginally effective. According to reports, chemotherapy has severe side effects, whereas surgery can only prevent local and regional recurrences. This necessitates the development of more efficient and cost-effective cancer treatment options, one of which is advancing anticancer nanoparticle research [2–4].

The essential oil of the *Zingiber zerumbet* (L.) Smith plant is the source of the active ingredient known as zerumbone [5]. Extensive studies on zerumbone's potential as an anticancer agent have revealed the molecule's cytotoxic effect against multiple cancer cell lines, including those derived from cholangiocarcinoma, lymphoblastic leukemia, ovarian, and renal tumors [6–9]. The formulation options for zerumbone are restricted by its poor solubility and bioavailability [10, 11].

The use of nanoparticles as drug carriers has great potential, especially for poorly water-soluble compounds [12]. Natural biopolymer chitosan has many desirable properties for nanoparticle production, including non-toxicity, biodegradability, and biocompatibility. As well as regulating drug release, incorporating chitosan into the formulation improved the medicinal compound's stability, solubility, and bioavailability. Drug loading and active component release profile improvements have resulted from modifying chitosan with various chemical agents, leading to enhanced interaction between drug and nanoparticle carriers [13]. Our group has recently investigated the feasibility of enclosing zerumbone in chitosan nanoparticles modified with oleic acid. The encapsulation efficiency of zerumbone was increased when oleic acid-modified chitosan nanoparticles were used instead of chitosan alone due to the hydrophobic moiety of the oleic acid [14].

This research aimed to investigate the delivery and the cytotoxic effect of zerumbone-loaded chitosan-oleic acid nanoparticles against breast cancer T47D cells using MTT and confocal scanning laser microscope.

MATERIALS AND METHODS

Materials

Materials used were obtained from Sigma Aldrich, including chitosan, oleic acid, (1-ethyl-3-(3-dimethyl aminopropyl)-carbodiimide HCl (EDC), glacial acetic acid pro analysis, ether, ammonium hydroxide, methanol, sodium tripolyphosphate (Na-TPP), ethanol pro analysis, DMSO, Tween 80, NaOH, acetonitrile (HPLC grade), methanol (HPLC grade), trypsin-EDTA solution, PBS (Phosphate Buffer Saline), culture media (RPMI), MTT, SDS 10%, HCl, tissue, annexin-V, RNase, propidium iodide, triton-X, dialysis membrane, acridine orange, and propidium iodide. Zerumbone was isolated and purified from the essential oil of *Zingiber zerumbet* (L.) Smith, in the laboratory of Pharmaceutical Chemistry, Faculty of Pharmacy, Universitas Muhammadiyah Surakarta.

Synthesis of nanoparticles

Nanoparticles (NPs) were made by dissolving oleic acid-chitosan (OAC) in 2.5 ml of 1% acetic acid solution and agitating the mixture for an entire night. The solution's pH was lowered to 4.8 with the help of 1.0 N NaOH. Zerumbone (Zer) was added to the mixture after being dissolved in DMSO. After 30 min of blending, Tween 80 was added. Drop by drop, Na-TPP solution was added while being thoroughly mixed.

Characterization of nanoparticles

The nanoparticles were characterized for their transmittance, particle size, polydispersity index (PI), zeta potential, encapsulation efficiency, and morphology. Solutions of zerumbone-loaded oleic

acid-chitosan nanoparticles (Zer-OAC-NPs) and oleic acid-chitosan nanoparticles (OAC-NPs) were introduced into the cuvette, and the transmittance was evaluated using UV spectrophotometry at 650 nm (Genesys 10S, Thermo Scientific). A Particle Size Analyzer (Horiba Scientific-100 SZ) assessed particle size, polydispersity index (PI), and zeta potential. The cuvette containing a 3 ml solution of Zer-OAC-NPs and OAC-NPs was then introduced into the PSA to measure its size and polydispersity at 25 °C and a scattering angle of 90°.

Encapsulation efficiency (EE) was determined by placing a 1.0 ml solution of Zer-OAC-NPs and OAC-NPs on a dialysis membrane, which was then placed in a conical tube, centrifuged at 2000 rpm for one hour, and then measuring the supernatant at the upper of the conical tube with reverse phase HPLC (Shimadzu) at a wavelength of 254 nm using column C18 (Cosmosil) with a length of 150. The encapsulation efficiency (EE) was determined as follows (eq. 1).

$$\%EE = \frac{\text{total zerumbone added} - \text{free zerumbone}}{\text{total zerumbone added}} \text{ X } 100\% \text{ ..... (eq. 1)}$$

The morphology of NPs was evaluated using TEM. The grid was soaked in a solution of Zer-OAC-NPs and OAC-NPs and allowed to dry for morphological analysis. Phosphotungstic acid (PTA) 2% with a pH of 7 was poured onto a grid and then examined using a Transmission Electron Microscope (JEOL JEM-1400).

Cytotoxic assay of zerumbone nanoparticles using the MTT method

After calculating cells with 10,000 cells/100 µl for each well, they were put into a 96-well plate, leaving three wells as medium controls, and cultured overnight in a CO_2 incubator so that the cells recovered after harvesting. Cells were incubated for 24 h with 100 µl solution containing Zer-OAC-NPs, OAC-NPs, and zerumbone isolates at a concentration series of 100; 50; 25; 12.5; 6.25; 3.125; 1.56 µg/ml per well with three replications. The plate containing cells was removed from the CO_2 incubator, and then the cell media was removed by inverting the plate 180 degrees over the discharge point and pressing it on a tissue. 100 µl of MTT solution was added to 5 mg/ml PBS and incubated for 2-4 h. A 10% SDS stopper in 0.1 N HCl containing 100 µl was added to the well after observing the cell status under an inverted microscope (Olympus CKX41); once a formazan has developed, it was wrapped in aluminum foil and incubated at room temperature overnight in a dark location. It was then placed into the ELISA reader (Elx 800 BioTech), and the absorbance of each well was measured with a wavelength range of 550-600 nm. The percentage of living cells was determined by calculating the absorbance (eq. 2) and then graphing the concentration log versus the percentage of living cells to obtain a linear regression equation (Y=BX+A). The IC_{50} was determined by substituting the value of Y with a value of 50% to obtain the value of X.

$$\% \text{ cells viability} = \frac{(\text{Absorbance of treatment} - \text{Absorbance of blank})}{(\text{Absorbance of control} - \text{Absorbance of blank})} \text{ x } 100\% \text{ .. (eq. 2)}$$

Apoptosis and cell cycle assay using flow cytometric method

Cells that had been 70-80% confluent were harvested, then cell calculations were carried out with $5x10^5$ cells/1000 µl for apoptosis assays and $1x10^6$ cells/1000 µl for cell cycle tests for each well. Cells were then transferred into a 6-well plate and incubated overnight so that the cells recovered after being harvested. Cells were then incubated for 24 h in a solution containing Zer-OAC-NPs and zerumbone isolates at a concentration of ½IC_{50} and IC_{50} of 1000 µl per well with three replications. The cell media were removed, 200 µl of trypsin-EDTA solution 0.25% were added to each well and incubated for 3 min. Cells were redispersed with up to 1 ml of MK medium in each well and were transferred to the conical. 500 µl PBS was added to the conical and spun at 600 rpm for five minutes. MK and PBS media were then removed. The pellets recovered were added 500 µl of cold PBS and were centrifuged at 600 rpm for 5 min. For cell fixation in the cell cycle assay, PBS is poured out with 500 µl of 70% alcohol at a rate of 1 drop/second per well. The mixture is left at room temperature for 30 min before being centrifuged at 600 rpm for 5 min, after which the alcohol is removed. 500 µl PBS was added and centrifuged at 2000 rpm for 3 min, then washed twice with PBS. The test substances were added. Annexin and propidium iodide (PI) reagents were used for apoptosis assays. The resulting cell suspension was treated with PI, RNase, and Triton-X reagents for cell cycle testing. Subsequently, after 30 min at room temperature, the cell suspension was transferred into the flowcyto-tube. Apoptosis induction readings and cell cycle analysis were conducted using the FACS Calibur flow cytometer.

Observation of cells using a confocal scanning laser microscope (CSLM)

Observation of cells was performed using a confocal scanning laser microscope (Carl Zeiss Axio) and double labeling. The double staining technique apoptosis test required $5x10^5$ cells/200 µl per well. Each cell was then put into 24 well plates filled with coverslips and treated for 3 to 30 min in an incubator so that the cells adhere to the coverslip. 800 µl of MK were added to the well, and the state of the cells was observed under the microscope to determine their distribution and was incubated overnight in an incubator. 1000 µl of Zer-OAC-NPs solution and zerumbone isolate were added at the IC_{50} per well, followed by 10 to 24 h of incubation. The coverslip was taken and then put on the object glass. A 10 µl solution of acridine orange-propidium iodide was dropped on the coverslip and observed under a confocal microscope.

Data analysis

Statistical analysis was conducted using SPSS version 23 with post hoc comparison one-way analysis of variance as opposed to Tukey's test. $P<0.05$ is regarded to be statistically significant.

RESULTS AND DISCUSSION

Synthesis of nanoparticles

Poor solubility in water and the inability to pass through the absorption barrier might reduce the bioavailability of medications or natural component molecules in the body. Drug delivery systems based on nanotechnology can significantly assist in overcoming formulations of medicines with low solubility in water and solvents [15]. The creation of nanoparticle pharmaceuticals permits increased release of the targeted system, enhanced solubility of hydrophobic medications, fewer adverse effects, and enhanced therapeutic efficacy. Encapsulation with micro-polymers or nanoparticles is one solution for maintaining bioactive substances' stability by extending their half-life. Zerumbone has a low solubility profile (1.296 mg/l at 25 °C) in water; to improve its solubility, zerumbone is encapsulated with an amphiphilic chitosan-oleic acid modification. The ionic gelation method can aid in reducing particle size; ionic gelation occurs when the amine group ($-NH_3^+$) of chitosan, which is positively charged, interacts with negatively charged groups on NaTPP such as $P_3O_5^-$dan $HP_3O_4^-$ [15].

Characterization of nanoparticles

The transmittance, particle size, polydispersity index, zeta potential, encapsulation efficiencies, and morphological appearance of Zer-OAC-NPs and OAC-NPs are determined. Table 1 displays the findings of the characterization of Zer-OAC-NPs and OAC-NPs.

Table 1: Characterization of chitosan-oleic acid nanoparticles (OAC-NPs) and chitosan-oleic acid zerumbone nanoparticles (Zer-OAC-NPs)

Parameters	OAC-NPs	Zer-OAC-NPs
Transmittance (%)*	99.13±0.5	99.90±0.1
Particle size (nm)*	83.36±0.9	116±12.03
Polydispersity index	0.70±0.01	0.73±0.60
Zeta potential (mV)*	52.66±1.00	34.40±0.43

Results show the average±SD of three replications. *denotes a significant difference between the chitosan-oleic acid nanoparticle group and the zerumbone-chitosan-oleic acid nanoparticle with a significance value ($P<0.05$).

The statistical tests revealed a significant difference between the Zer-OAC-NPs group and the OAC-NPs regarding the transmittance, particle size, and zeta potential, but not the polydispersity parameter. The results were similar to a previous study that reported the curcumin nanoparticles contained in chitosan-oleic acid modified poly-lactic-glycolic acid (Cur-CS-OA-PLGA) and chitosan-oleic acid nanoparticles modified poly-lactic-glycolic acid (CS-OA-PLGA) have different size parameters, zeta potential, and polydispersity index. Nonetheless, the polydispersity index of OAC-NPs and Zer-OAC-NPs indicated monodispersed nanoparticles [16].

According to Rahmawanty *et al.*, Zer-OAC-NPs were larger than OAC-NPs based on particle size measurements. In her investigation, there were changes in particle size between tripolyphosphate suspensions with varying compositions of snakehead fish powders, with the suspensions containing a greater proportion of snakehead fish powders [17]. Many have bigger particle sizes than suspensions that contain less powder. The particle size was most likely the result of the combustion of the gel mass on the particle surface. The difference in size between Zer-OAC-NPs and OAC-NPs was presumably owing to the coating or encapsulating of the chitosan-oleic acid mass on the surface of the zerumbone particles.

The pH of the medium affects the zeta potential; additional considerations were the ionic strength, the concentration of the additive, and the temperature [18]. The zeta potential of Zer-OAC-NPs was less than that of OAC-NPs, consistent with other research findings. In previous research, zinc pectinate nanoparticles in NaCl medium, including diltiazem hydroxide, had a lesser potential zeta value than zinc pectinate nanoparticles in NaCl media without diltiazem hydroxide and Zn pectinate nanoparticles with diltiazem hydroxide in aqueous media. The variation in zeta potential was influenced by changes in the nanoparticle system's composition and the number of cations and anions [19]. The addition of zerumbone-DMSO can thereby influence the zeta potential of Zer-OAC-NPs, as can be deduced.

Zerumbone of 92.43±31.731% can be encapsulated in chitosan-oleic acid nanoparticles according to the measurement of efficiency encapsulation (EE). Similarly, Rahman *et al.* demonstrated that zerumbone (0.4% w/v) might be contained in lipid carriers (hydrogenate palm oil, olive oil, and lipoid S100) with a 7:3:3 (Zer-NLC) ratio with an EE of 99.03% [20]. In general, the solubility of the drug would rise in lipid liquids relative to lipid solids as EE increases. In addition, the polymer-drug ratio was one of the factors that might influence EE. The EE can drop if the polymer-drug ratio increases and it can increase if the amount of polymer is raised proportionally to the increase in active compounds [21].

Fig. 1 depicted the outcomes of morphological observations using TEM. In TEM morphological investigations, both Zer-OAC-NPs and OAC-NPs appear spherical, except that Zer-OAC-NPs have a core structure and a thin surface surrounding them. The same holds for the previous research, in which nanocapsules exhibited compact structures compared to empty nanoparticles.

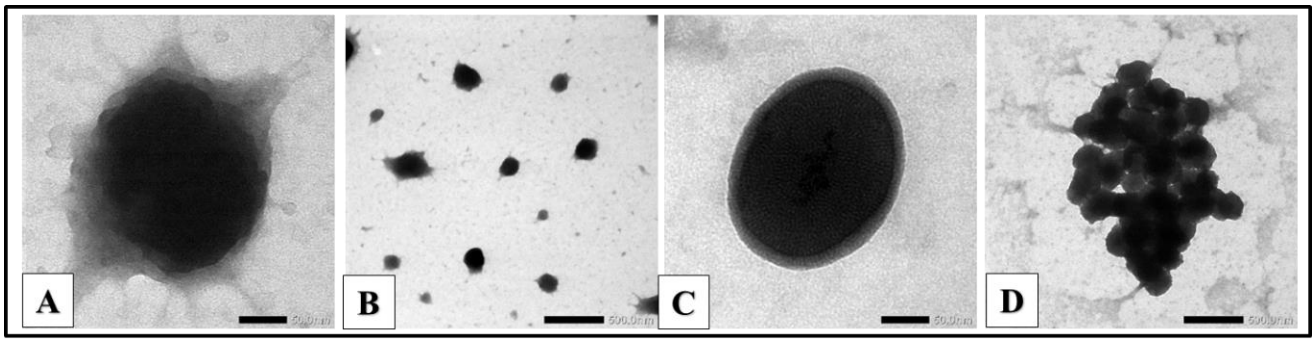

Fig. 1: Morphological sightings using TEM. Morphology of chitosan-oleic acid nanoparticles with a magnification of 150,000x (A) and 15,000x (B) and zerumbone-loaded chitosan-oleic acid nanoparticles with a magnification 150,000x (C) 15,000x (D)

Cytotoxicity of nanoparticles against T47D cells

The MTT method is based on reducing the yellow salt of tetrazolium MTT (bromide of 3-(4,5-dimethylthiazol-2-yl)-2,5-diphenyl-tetrazolium) by the reductase system. Tetrazolium succinate, part of the respiration cycle in the mitochondria of living cells, creates water-insoluble purple crystals of formazan. These colored crystals are dissolved by adding a stopper reagent (detergent), and their absorbance is then measured using an ELISA reader. The intensity of the resulting purple hue is proportional to the number of live cells present. Hence, if the intensity of purple increases, the number of live cells increases.

T47D cells were utilized and frequently used in *in vitro* cancer research because they are simple to manipulate, have unlimited replication capacity, have high homogeneity, and can be changed in the event of contamination. T47D cells that were alive or before treatment would appear connected to the bottom of the well with an oblong shape, but T47D cells that have died after treatment will float and have a sphere shape. Fig. 2 depicted the outcomes of observations of T47D cells using an inverted microscope.

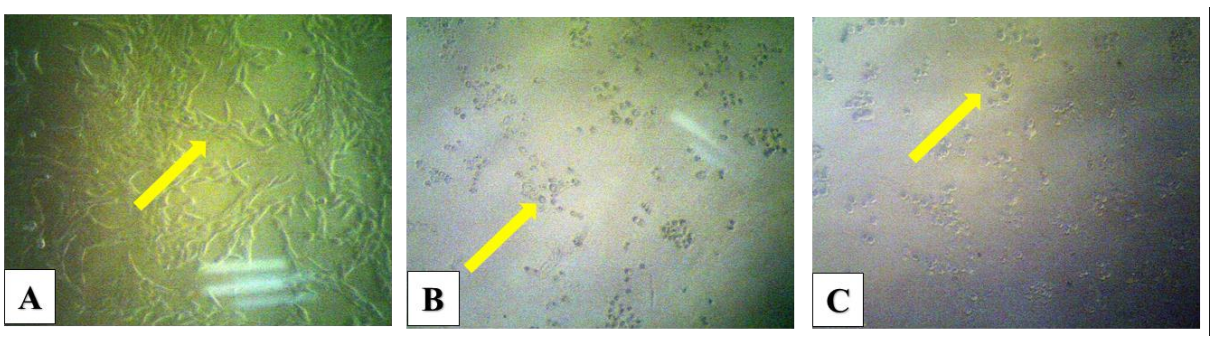

Fig. 2: Morphological observations of T47D cells with a magnification of 100x; T47D cells before treatment (A) T47D cells after Zer-OAC-NPs treatment 12.5 µg/ml (B) T47D cells after receiving zerumbone isolate treatment 12.5 µg/ml (C)

According to Geran *et al.*, compounds has IC_{50} of 20 µg/ml are included in the active category, whereas IC_{50}>500 µg/ml is included in the inactive category. Cytotoxic assays reveal that the anticancer activity of Zer-OAC-NPs and zerumbone isolates falls into the active category, while OAC-NPs fall into the inactive category (table 2).

Table 2: Cytotoxic test results of chitosan-oleic acid nanoparticles, zerumbone isolates, and chitosan-oleic acid zerumbone nanoparticles against T47D cells

Parameters	OAC-NPs	Zer-isolates	Zer-OAC-NPs
IC_{50} (µg/ml)	$3.461x10^{9}$±$3.004 x10^{9}$	20.762±1.912	11.241±2.086

Results show the average of three replication. There is a significant difference between the chitosan-oleic acid nanoparticle group, zerumbone isolate, and zerumbone-chitosan-oleic acid nanoparticles with significance values (P<0.05).

The lower the IC_{50}, the greater the compound's cytotoxic action. This study determined that Zer-OAC-NPs had an IC_{50} 46% lower than that of zerumbone isolates, with a significance value (p<0.05), so it can be concluded that Zer-OAC-NPs can affect the anticancer activity of zerumbone. However, this result differs from the research previously that demonstrated the anticancer efficacy of zerumbone by comparing the IC_{50} values of free zerumbone and zerumbone-nanostructured lipid carrier (Zer-NLC), which is 11.87±0.17 and 12.5±0.1 µg/ml, respectively. The formulation of zerumbone nanoparticles by chitosan-oleic acid encapsulation rather than lipid encapsulation can impact the anticancer activity of zerumbone [21].

Observation of apoptosis and cell cycle

Apoptosis is a planned cell death mechanism characterized by morphological and biochemical alterations. The apoptosis test investigated whether zerumbone isolates and Zer-OAC-NPs at IC_{50} and $1/2IC_{50}$ induced apoptosis in T47D cells. Annexin attached to phosphatidylserine on the surface of apoptotic cells, and PI was utilized to differentiate between live cells, apoptosis, and necrosis [22].

In this experiment, Zer-OAC-NPs with a concentration of 1/2 IC_{50} and IC_{50} showed a tiny percentage of apoptosis, i. e., 1.59±2.60% and 0.160±0.269% in initial apoptosis, as well as 0.48±0.76% and 0.16±0.26% in late apoptosis, with no significant difference between cell control, Zer-OAC-NPs, and the zerumbone isolate. The standard deviation appeared to be more extensive than usual. This was because the majority of cells perished owing to necrosis. Fig. 3 depicted the outcomes of the apoptosis induction experiment. In contrast to the research conducted by Rahman *et al.*, the apoptosis induction test with 24 h of treatment showed that Zer-NLC at IC_{50} could induce apoptosis of Jurkat cells by 3.45±0.11 in initial apoptosis and 2.66±0.11 in the final apoptosis with significance values between the cell control group and Zer-NLC (p<0.05), and no necrosis cells were found.

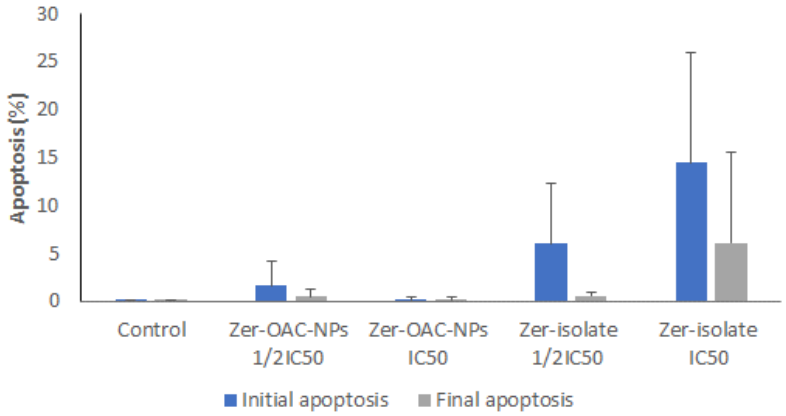

Fig. 3: The results of the apoptosis induction experiment with treatment for 24 h. Statistical analysis shows a significance value (p>0.05)

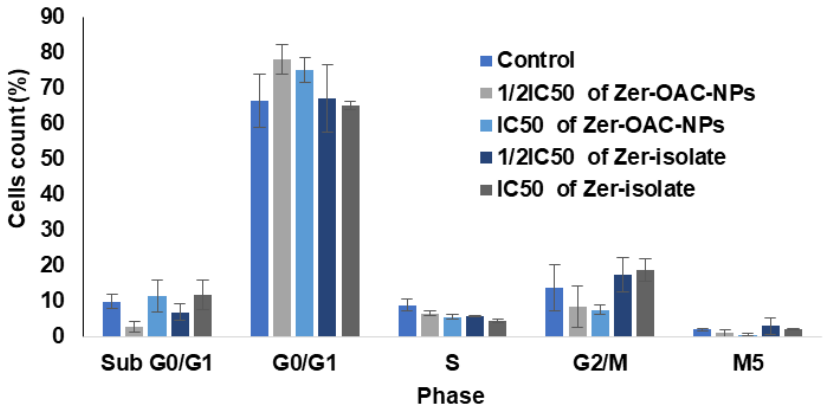

Fig. 4: The results of the observation of the cell cycle test with a 48 h treatment. Statistical Analysis shows the significance value (P>0.05) of each treatment and each phase except in phase S

The objective of the cell cycle test was to determine in which phase T47D cells can re-enter the cell cycle following treatment with zerumbone isolates and zerumbone-chitosan-oleic acid nanoparticles at concentrations of $1/2IC_{50}$ and IC_{50} (fig. 4). The cell cycle observations on zerumbone isolate treatment of IC_{50} concentration showed a decrease in the percent of T47D cells living in the G0/G1 phase compared to cell control was subsequently found accumulation or increase in the G2/M phase in the treatment of IC_{50} zerumbone isolates compared to cell control. It can be concluded that zerumbone induced G2/M arrest of T47D cells. However, statistical analysis showed (P>0.05), which means that there is no significant difference between control and zerumbone isolate treatment. The cell arrest occured in the G0/G1 phase, which was indicated by a decrease in the percent of live T47D cells in the M5 phase compared to cell control (P>0.05). In contrast with the research conducted previously, both free zerumbone and Zer-NLC induced G2/M arrest characterized by G1 phase, which subsequently there was an accumulation or increase in phase G2/M with statistical analysis (P<0.05). It can be concluded that the formulation of zerumbone nanoparticles with chitosan-oleic acid encapsulation can also affect cell arrest of zerumbone while the difference profile of G2/M arrest between zerumbone isolates of IC_{50} concentration and zerumbone isolates of concentration $1/2IC_{50}$ can occur due to the difference in the concentration [23].

A confocal microscope allows us to see both cells and nanoparticle drugs on an intracellular scale with the help of dye reagents. In addition, the confocal microscope can also determine the apoptosis induction profile of a nanoparticle drug against cells and can be used to determine changes in cell structure after treatment. Cells stained with fluorescence dye reagents can be seen in distribution; living cells or cells that have undergone initial apoptosis will appear green, cells in the final apoptosis will be orange/yellow, whereas the cells that undergo necrosis will appear red. The results of morphological observations of T47D cells using a confocal microscope can be seen in fig. 5 and the distribution of T47D cells for each treatment can be seen in fig. 6.

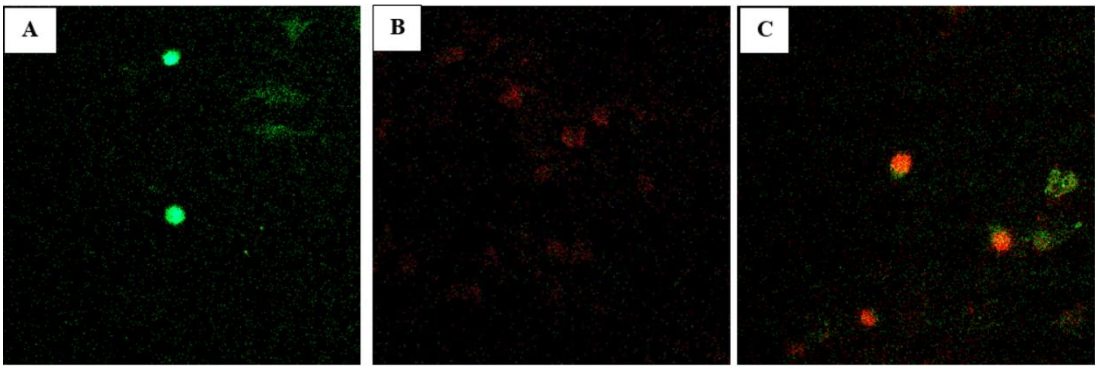

Fig. 5: Morphological observations of T47D cells using a confocal microscope at λ 565 and 617 nm with treatment for 48 h. Cell control (A), zerumbone isolates (B), and zerumbone-chitosan-oleic acid nanoparticles (C)

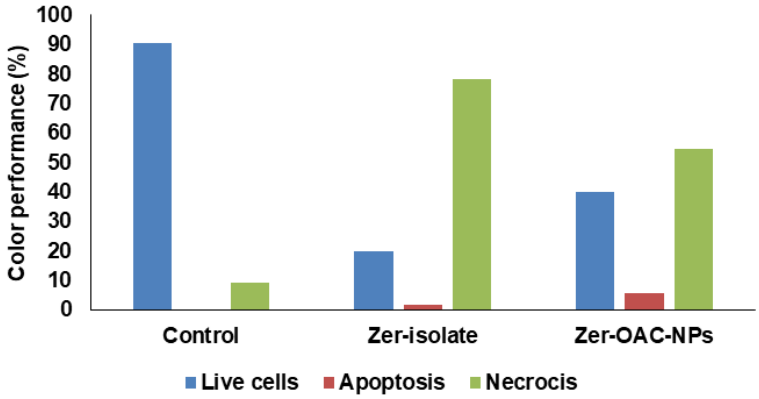

Fig. 6: The percentage of color performance of the distribution of T47D cells; results show the percent intensity of green, yellow, and red colors

The results of morphological observations using a confocal microscope showed the dominance of living T47D cells in cell control which was blinded by the dominance of green luminescence in fig. 5. On treatment with zerumbone isolates, fig. 5. dominated by red which shows the dominance of T47D necrosis cells while in the Zer-OAC-NPs treatment there is a distribution of green, yellow and red luminescence which indicated the presence of a distribution of live T47D cells, apoptosis T47D cells and necrosis T47D cells. Color performance analysis showed that the Zer-OAC-NPs treatment was able to induce 5.5 % more apoptosis than the zerumbone isolate treatment, which was only 0 1.60% while in the cell control group, there was no cell apoptosis and was dominated by live T47D cells by 90.60%. This is also the case with the study cells with Zer-NLC treatment for 48 h showed a distribution of green, yellow and red color luminescence compared to the cell control group, which was dominated only by green luminescence. In addition, changes in cell structure after treatment could also be seen in this study; cells with Zer-NLC treatment for 48 h showed changes in cell structure such as blebbing, chromatin condensation and nuclear margination [23].

CONCLUSION

The results of cytotoxic analysis showed significant values between Zer-OAC-NPs and zerumbone isolates (P<0.05) with an IC_{50} value of Zer-OAC-NPs of 11.241±1.703 µg/ml. Apoptosis test showed that Zer-OAC-NPs of IC_{50} and $1/2IC_{50}$ were able to induce T47D cell apoptosis by 1.597%±2.603% and 0.160%±0.269% in initial apoptosis and 0.483%± 0.759% and 0.160%±0.260% in final apoptosis with significance values between Zer-OAC-NPs,

zerumbone isolates and cell control of (P>0.05) and showed G 0/G1 *arrest* with significance values between Zer-OAC-NPs, isolates zerumbone and cell control of (P>0.05).

This study also observed the T47D cells under confocal microscope through color intensity performance analysis showed that Zer-OAC-NPs treatment could induce 5.5% more apoptosis than zerumbone isolate treatment, which was only 1.60%, while in the cell control group there was no cell apoptosis.

ACKNOWLEDGEMENT

The author would like to thank LPPM Universitas Muhammadiyah Surakarta for funding this research through the scheme of PINPRU.

AUTHORS CONTRIBUTIONS

All authors discussed the results and contributed to the final manuscript. Conceptualization and funding acquisition: EW; performing the experiment and data collection: ZM and SS; data analysis: IK and MD.

CONFLICT OF INTERESTS

The authors declared at no conflict of interest should arise concerning the authorship of this research article.

REFERENCES

1. Sung H, Ferlay J, Siegel RL, Laversanne M, Soerjomataram I, Jemal A. Global cancer statistics 2020: GLOBOCAN estimates of incidence and mortality worldwide for 36 cancers in 185 countries. CA Cancer J Clin. 2021;71(3):209-49. doi: 10.3322/caac.21660, PMID 33538338.
2. Waks AG, Winer EP. Breast cancer treatment: a review. JAMA. 2019 Jan 22;321(3):288-300. doi: 10.1001/jama.2018.19323, PMID 30667505.
3. Yuliani R, Syahdeni F. Cytotoxicity of ethanolic extract of papaya leaves (Carica papaya) and its fractions on T47D cells. Pharmacon J Farmasi Indones. 2020;17(1):17-23. doi: 10.23917/pharmacon.v17i1.10760.
4. Nabilla II, Indrayudha P. Aktivitas sitotoksik ekstrak etanol fraksi etanol etil-asetat dan heksana kulit jeruk purut (Citrus hystrix dc.) terhadap sel kanker payudara T47D. Pharmacon J Farmasi Indones. 2019 Jul 15;16(1):11-7. doi: 10.23917/pharmacon.v16i1.8173.
5. Srivastava AK, Srivastava SK, Shah NC. Essential oil composition of Zingiber zerumbet (L.) Sm. From India. J Essent Oil Res. 2000 Sep 1;12(5):595-7. doi: 10.1080/10412905.2000.9712165.
6. Chan ML, Liang JW, HSU LC, Chang WL, Lee SS, Guh JH. Zerumbone a ginger sesquiterpene, induces apoptosis and autophagy in human hormone-refractory prostate cancers through tubulin binding and crosstalk between endoplasmic reticulum stress and mitochondrial insult. Naunyn Schmiedebergs Arch Pharmacol. 2015;388(11):1223-36. doi: 10.1007/s00210-015-1152-z, PMID 26246051.
7. Hanwar D, Suhendi A, Trisharyanti I, Santoso B, Safitri M. Secondary metabolite profile analysis of lempuyang emprit extract by gas chromatography-mass spectroscopy. University Research Colloquium. 2015;1:158-66.
8. Dai M, Fadhilah A, Rahmawati J, Forentin AM, Usia T, Maryati M. T47D cell-inhibiting Indonesian medicinal plants and active constituents of Alpinia galanga rhizome. Pharmacogn Mag. 2018;14(56):359. doi: 10.4103/pm.pm_259_17.
9. Shamoto T, Matsuo Y, Shibata T, Tsuboi K, Nagasaki T, Takahashi H. Zerumbone inhibits angiogenesis by blocking NF-κB activity in pancreatic cancer. Pancreas. 2014 Apr 1;43(3):396-404. doi: 10.1097/MPA.0000000000000039, PMID 24622069.
10. Ibanez MD, Sanchez Ballester NM, Blazquez MA. Healthy zerumbone: from natural sources to strategies to improve its bioavailability and oral administration. Plants (Basel). 2022 Dec 20;12(1):5. doi: 10.3390/plants12010005, PMID 36616138.
11. Hassan MM, Mohammed AF, Elamin KM, Devkota HP, Ohno Y, Motoyama K. Improvement of pharmaceutical properties of zerumbone a multifunctional compound using cyclodextrin derivatives. Chem Pharm Bull (Tokyo). 2020 Nov 1;68(11):1117-20. doi: 10.1248/cpb.c20-00621, PMID 33132380.
12. Raikar PR, Dandagi PM. Functionalized polymeric nanoparticles: a novel targeted approach for oncology care. Int J App Pharm. 2021;13(6):1-18. doi: 10.22159/ijap.2021v13i6.42714.
13. Garg U, Chauhan S, Nagaich U, Jain N. Current advances in chitosan nanoparticles based drug delivery and targeting. Adv Pharm Bull. 2019 Jun;9(2):195-204. doi: 10.15171/apb.2019.023, PMID 31380245.
14. Wikantyasning ER, Andasari SD, Da'i M, Nabila A. Nanoencapsulation of zerumbone in oleic acid modified chitosan nanoparticles. ACM Int Conf Proceeding S. 2017:105-9. doi: 10.1145/3155077.3155097.
15. Kesharwani SS, Bhat GJ. Formulation and nanotechnology-based approaches for solubility and bioavailability enhancement of zerumbone. Medicina (Kaunas). 2020;56(11):557. doi: 10.3390/medicina56110557, PMID 33114101.
16. Miele D, Rossi S, Sandri G, Vigani B, Sorrenti M, Giunchedi P. Chitosan oleate salt as an amphiphilic polymer for the surface modification of poly lactic glycolic acid (PLGA) nanoparticles preliminary studies of mucoadhesion and cell interaction properties. Mar Drugs. 2018 Nov 15;16(11):447. doi: 10.3390/md16110447, PMID 30445668.
17. Rahmawanty D, Anwar E, Bahtiar A. Utilization of cross linked chitosan with tripolyphosphate as an excipient for haruan fish gel. J Ilm Kefarmasian Indones. 2015;13(1):76-81.
18. Kumar A, Dixit CK. Methods for characterization of nanoparticles. Inadv Nanomed Deliv Ther Nucleic Acids. 2017:43-58. doi: 10.1016/B978-0-08-100557-6.00003-1.
19. Bhattacharjee S. DLS and zeta potential-what they are and what they are not? J Control Release. 2016 Aug 10;235:337-51. doi: 10.1016/j.jconrel.2016.06.017, PMID 27297779.
20. Rahman HS, Rasedee A, Abdul AB, Zeenathul NA, Othman HH, Yeap SK. Zerumbone-loaded nanostructured lipid carrier induces G2/M cell cycle arrest and apoptosis via mitochondrial pathway in a human lymphoblastic leukemia cell line. Int J Nanomedicine. 2014 Jan 16;9:527-38. doi: 10.2147/IJN.S54346, PMID 24549090.
21. Mohamad NE, Abu N, Rahman HS, KY H, HO WY, Lim KL. Nanostructured lipid carrier improved *in vivo* anti-tumor and immunomodulatory effect of zerumbone in 4T1 challenged mice. RSC Adv. 2015;5(28):22066-74. doi: 10.1039/C5RA00144G.
22. Carneiro BA, El Deiry WS. Targeting apoptosis in cancer therapy. Nat Rev Clin Oncol. 2020 Jul;17(7):395-417. doi: 10.1038/s41571-020-0341-y, PMID 32203277.
23. Hosseinpour M, Abdul AB, Rahman HS, Rasedee A, Yeap SK, Ahmadi N. Comparison of the apoptotic inducing effect of zerumbone and zerumbone loaded nanostructured lipid carrier on human mammary adenocarcinoma MDA-MB-231 cell line. J Nanomater. 2014;2014(1):182. doi: 10.1155/2014/742738.